Roles of cytokines in modulating Trypanosoma brucei rhodesiense infection outcomes in vervet monkeys

Vincent Adung'a

vowino@gmail.com

Egerton University

Clara Jebet

Egerton University

Thuita John

Meru University of Science and Technology

Daniel Masiga

International Centre of Insect Physiology and Ecology https://orcid.org/0000-0001-7513-0887

Oidho John

Biotechnology Research Institute - Kenya Agricultural and Livestock Research Organisation

Mark Field

University of Dundee

Enock Matovu

Makerere University

Benedict Orindi

Kenya Medical Research Institute

Article

Keywords:

Posted Date: July 24th, 2024

DOI: https://doi.org/10.21203/rs.3.rs-4609810/v1

Additional Declarations:

"This study involving non-human primate model of sleeping sickness is under a broader study entitled "Expression Profiling of African Trypanosomes in Mouse and Primate Hosts" that was approved by Institutional Animal Care and Use Committee (IACUC) of the then Trypanosome Research Centre - Kenya Agricultural Research Institute (TRC-KARI) currently Biotechnology Research Institute - Kenya Agricultural and Livestock Research Organisation (BRI-KALRO). "

There is **NO** Competing Interest.

Roles of cytokines in modulating *Trypanosoma brucei rhodesiense* infection outcomes in vervet monkeys

Jebet Clarah [a], Thuita Kibuthu John [b,d], Masiga Daniel [c], Benedict Orindi [e], Oidho John [b], Mark C. Field [f,g], Enock Matovu [i], Adung'a Vincent Owino [a,c *]

[a] *Department of Biochemistry and Molecular Biology, Egerton University, P. O Box, 536-20115, Egerton, Kenya*

[b] *Biotechnology Research Institute - Kenya Agricultural and Livestock Research Organisation, Chemotherapy Division, Primate Section, P.O Box, 362-00902, Kikuyu, Kenya*

[c] *International Centre of Insect Physiology and Ecology, P. O Box, 30772-000100, Nairobi, Kenya*

[d] *Department of Animal Sciences, School of Agriculture and Food Sciences, Meru University of Science and Technology, P.O Box, 972-60200, Meru, Kenya*

[e] *Department of Public Health and Primary Care, Leuven Biostatistics and Statistical Bioinformatics Centre, Kapucijnenvoer 35, Blok D, Bus 7001, B-3000, Leuven, Belgium*

[f] *School of Life Sciences, University of Dundee, Dundee, Scotland, UK*

[g] *Institute of Parasitology, Czech Academy of Sciences, České Budějovice, Czech Republic*

[i] *Department of Veterinary Parasitology and Microbiology, Faculty of Science, Makerere University, Kampala, Uganda*

***Corresponding author.** Department of Biochemistry and Molecular Biology, Egerton University. P. O Box 536-20115, Egerton, Kenya. E-mail addresses: vincent.adunga@egerton.ac.ke or vowino@gmail.com (VOA)

Abstract

Human African trypanosomiasis (HAT), caused by *Trypanosoma brucei rhodesiense,* remains a threat in east and southern African regions. The disease is widely categorised as acute, but often presents varying clinical outcomes that could also be considered as chronic. Although the mechanisms underpinning these variable clinical dynamics are poorly understood, host and parasite factors or both have been suggested. Here we assessed the roles of host cytokines in disease progression using a non-human primate (NHP), vervet monkey (*Chlorocebus aethiops*) model of HAT. We quantified the levels of eight cytokines, including TNF-α, IFN- γ, IL-10, IL-6, IL-12 and IL-1 β, the brain injury biomarker S100β, clinical data and compared acute and chronic infections. As expected, cytokine levels in both infected groups were significantly higher than uninfected controls ($P<0.05$). IL-12, IL-6 and IL-1β cytokines were significantly elevated ($p < 0.05$) in early-stage disease which extended from infection to the onset of late stage disease at a median (range) time of 16 (8-24) and 16 (12-28) dpi for acute and chronic strains respectively. IL-1β, IL-6, IL-12 and IL-10 are implicated in pro- and counter inflammatory responses and their modulation. *C. aethiops* infected with KETRI 3801 died with a mean survival time of 28 days compared to KETRI 3928 with a mean survival time of 95 days. In addition, CSF parasite and WBC levels were higher in KETRI 3801 as compared to KETRI 3928 infections. We conclude that cytokines play a role in modulating disease progression and severity in a NHP model of *T. b. rhodesiense* HAT. Further, we validate the cyclic vervet monkey model of HAT, enhancing its utility for disease pathogenesis studies. These results are important in investigating host-pathogen interactions to unravel varying infection outcomes.

1. Introduction

Human African trypanosomiasis (HAT), also known as sleeping sickness, is a neglected tropical disease (NTD) caused by two subspecies of the protozoan parasite *Trypanosoma brucei*, *T. b. gambiense* affecting west and central Africa and *T. b. rhodesiense* affecting east and southern Africa. Both are transmitted by infected blood sucking tsetse flies (genus *Glossina*). HAT is a focal disease endemic in 36 countries of sub-Saharan Africa and affects some of the world's poorest populations, with an estimated 55 million people at risk of infection and 3 million living in moderate to high-risk areas[1-3], *albeit* that the number of HAT cases reported in 2019 and 2020 were 992 and 663 respectively, ideating that the human disease has come under control[2]. During 2017-2018, reported Rhodesian HAT represented 2% of the total HAT cases while in 2018-2020, Rhodesian HAT represented 13% of the total number[2,4]. Therefore, despite highly successful campaigns to bring down case numbers, HAT remains a public health threat in sub-Saharan Africa.

Rhodesian HAT is a zoonotic disease with livestock and wildlife as reservoirs. The disease has been reported in non-endemic countries, imported through travellers visiting areas of high transmission; among the latest a case from India[5]. The number of cases from non-endemic regions during the 2011-2020 period was 16, with 71% of the cases caused by *T. b. rhodesiense* and 29% by *T. b. gambiense*[2]. The disease is categorised as acute, with fast progression to late stage and ultimate death if not detected and treated early.

Previous pathogenicity studies of *T. b. rhodesiense* isolates have indicated variation in disease progression and virulence. Recently, differences in survival times with various categories of pathogenicity have been described from small rodent model studies[6,7], and which are consistent with findings that clinical Rhodesian HAT virulence increased northwards of the eastern and southern African region, albeit that the rodent infection model is far removed from the human immune system. Significantly, patients manifest acute and chronic infection despite all being infected with strains of *T. b. rhodesiense*[8]. The mechanism behind this clinical variance is unclear, but is likely associated with host and/or pathogen factors. Elucidation of the roles of primate host immune factors in mediating outcomes of *T. b. rhodesiense* infection is essential for understanding the varied clinical outcomes in natural HAT cases, but remains unexplored.

Cytokines are signalling molecules produced by immune cells and which play critical roles in the immune response, including towards *T. brucei* infection[9]. Cytokines regulate the proliferation, differentiation and maturation of immune cells and facilitate communication between immune cells. Cytokine dysregulation is associated with disease progression and

severity in HAT[8-11], based on material from clinical HAT cases (patients) and are, for the most part, limited in terms of accurate determination of disease onset, making the understanding of disease progression challenging. To address these issues, and specifically the lack of data from a primate model and controlled infection, we used the non-human primate (NHP) vervet monkey model of HAT, which closely mimics human disease[12]. We report on the association between cytokine production and the modulation of *T. b. rhodesiense* infection progression and disease outcomes.

2. Materials and Methods

2.1. Samples

Archived vervet monkey plasma and CSF samples were collected as described[12], with modifications. Briefly, two groups of four animals each were infected with *T. b. rhodesiense* strains, KETRI 3801 or KETRI 3928 that lead to acute and chronic infections respectively. A third group of four monkeys were uninfected controls. Animals infected with KETRI 3801 included numbers 708 (F), 701 (F), 709 (M) and 704 (M), monkeys infected with strain KETRI 3928 were 710 (F), 719 (F), 699 (M) and 715 (M), and uninfected monkeys were 703 (F), 717 (F), 705 (M) and 706 (M); M and F represent male and female respectively. Infection was mediated by a single bite from a tsetse fly confirmed to be infected with *T. b. rhodesiense,* as described[12]. Plasma samples were collected every four days until extremis, while CSF was collected from day eight post infection (pi) and after four days thereafter until extremis. Strain biodata and sampling regime are shown in Figure 1. Clinical data for the monkeys including parasitemia (in antilog to base 10), CSF white blood cell (WBC) counts, packed cell volume (PCV), weight, temperature, survival time and food consumption were retrieved from our archive and analysed. Plasma and CSF samples from three animals per cohort were used for cytokine analysis.

2.2. Immune factors

2.2.1. Cytokines assayed

Eight immune factors associated with varying African trypanosome infection outcomes in various HAT models[9,10,13-15] were considered. These include INF-γ, TGF-1β, TNF-α, IL-1β, IL-6, IL-10, IL-13 and IL-12. Also considered is S100β, a serum biomarker for brain injury suggested as a marker for neuronal and blood-brain barrier (BBB) damage, making it a potential HAT staging biomarker[16-18].

2.1.2. Sample preparation and standards

Cytokine ELISA kits from U-Cytech biosciences (Utrecht, Netherlands) were used to quantify monkey TNF-α, IFN- γ, IL-10, IL-6, IL-12, IL-13 and IL-1β cytokines in both plasma and CSF, and has been applied in others studies[19-21]. ABclonal Technology kits (Massachusetts, U.S.A.) were used to assay monkey TGF-1β and S100β in CSF, and have been applied elsewhere[16-18]. Samples (500 µl) were aliquoted into eppendorf tubes to avoid freeze-thaw cycles. For U-Cytech biosciences kits, 1/20 volume of cytokine stabilisation buffer (CSB) was added to samples prior to subsequent dilutions. Additionally, 10 µl of balance solution was added to every 100 µl of diluted samples according to the ABclonal Technology protocol. To generate a standard curve, a seven-fold serial dilution of standards in dilution buffer were prepared, and the dilution buffer was used as the blank.

2.2.2. Cytokine assays

The U-Cytech biosciences solid phase sandwich ELISA protocol was followed as per manufacturer's instructions. Optical densities (ODs) of each well was read at 450nm using Stat Fax 3200 Microplate Reader (GMI, Minnesota, USA). Each sample was measured in triplicate. Incubation at 37 °C was done using MB100-4A microplate shaker incubator (Mrc ltd, Holon, Israel), while incubation at 4 °C was done in ALB fridge (ALB Service Pty Ltd, West Burleigh, Australia).

The ABclonal Technology protocol required 100 µl of diluted sample added to the antibody coated wells. 50 µl of the enzyme solution were added and mixed. Plates were covered, incubated 37°C for 1 hr and thereafter washed three times with wash buffer. This was followed by addition of 50 µl of substrate A and another similar amount of substrate B, covered and incubated at RT for 20 mins. 50 µl of the stop solution were added into each well and the ODs immediately read at 450nm using Stat Fax 3200 Microplate Reader (Awareness Technology Inc, Palm City, Florida, USA).

2.3. Statistical analyses

To monitor differences in cytokine levels over time between monkeys infected with the different strains of *T. b. rhodesiensie*, a generalised additive mixed model (GAMM) was used, with monkeys included in the model as a random effect. GAMM allowed us to model the highly non-linear profiles over time[22]. Explanatory variables included strain (group) which entered the model (parametrically) as a fixed effect, time (days post infection) as a nonparametrically smoothed function, and time by strain smoothed term to allow each strain group to evolve differently over time. The uninfected group was taken as the reference against which other groups were compared. GAMM was used to allow the inclusion of

nonparametric smooth functions to model highly nonlinear trends in the data. GAMMs measure nonlinearity using the effective degrees of freedom (edf) of the smoothing term; an edf equal to 1 implies a linear function and the higher the edf the more nonlinear the function. GAMM was fitted using the 'gamm' function in 'mgcv' package[23]. This model was fitted separately for each cytokine using plasma data. Plasma data were analysed for six cytokines including IFN-γ, TNF-α, IL-10, IL-6, IL-12, and IL-1β. Plasma IL-13 and CSF levels for all the cytokines except TGF-1β and S100β, which exhibited no statistical significant alterations over the course of infection, and were not subjected to statistical analyses. All tests were performed at 5% significance level. Median survival times (and associated interquartile range, IQR) were estimated using Kaplan-Meier curves[24], and the curves compared across strains using Log rank test. GAMM analyses were performed using R version 3.6.1[25] and survival analysis was performed using Stata v15.1 (StataCorp, College Station, TX).

3. Results

3.1. Pathogenicity of *T. b. rhodesiense* strains in vervet monkey

Varying infection outcomes observed from infections with the KETRI 3801 and KETRI 3928 strains have been reported previously in both vervet monkey and mouse models[6,7,12]. Here, a trypanosome chancre was observed in 1 of 4 monkeys (708) infected with KETRI 3801 and 2 of 4 monkeys (699 and 715) infected with KETRI 3928. The pre-patent period was median 6.0 dpi (range: 6 - 6) and 6.3 dpi (range: 6 - 7) days for KETRI 3801 and KETRI 3928 infections respectively (Table 1). Following pre-patency, KETRI 3801 parasitaemia rose to a peak of antilog 8.7 parasites/mL by 12 dpi before falling; a second and third peak were observed before animals reached extremis (Figure 1 and Figure 2). In contrast, KETRI 3928 parasitaemia rose to a lower magnitude peak of antilog 7.8 by 8 dpi (Figure 2). Parasitaemia continued to fluctuate between antilog 6.1 and 7.8 parasites/mL throughout the infection (Figure 2). Overall, a higher parasitaemia was observed in monkeys infected with KETRI 3801 than in those infected with KETRI 3928 strain (Figure 2).

Animals infected with KETRI 3801 survived for shorter times compared to those infected with KETRI 3928. The median survival time was 28 (interquartile range, IQR 23 – 34) days for KETRI 3801, 95 (IQR 57 – 115) days for KETRI 3928, and 120 (IQR 120 – 120) days for uninfected monkeys (see Figure 1 and Figure 2B); clinical monitoring of the uninfected monkeys was terminated at 120 days without a requirement for them to attain the extremis condition. Compared to KETRI 3928 infected monkeys, time to death is about a third in

KETRI 3801 infections (HR=2.48, 95%CI: 1.42-4.30), but between KETRI 3928 infections and uninfected controls was not statistically significantly different (p=0.0704) (HR=0.66, 95%CI: 0.42-1.00) (See Figure 2C). As in previous studies[7,12], these data indicate that KETRI 3801 causes an acute infection compared to the chronic and milder KETRI 3928 infections.

Table 1. Changes in clinical and parasitological parameters in vervet monkeys cyclically infected with two strains of *T. b. rhodesiense* KETRI 3801 and KETRI 3928 parasites.

Clinical and parasitological parameters	Control	KETRI 3801	KETRI 3928
Proportion of monkeys with chancre	N/A	1/4	2/4
Pre-patent period (days)	N/A	6.0 (6 - 6)	6.3 (6 - 7)
Time to first peak parasitaemia in dpi (parasite load/mL at first peak)	N/A	12 (antilog 8.7/mL)	8 (antilog 7.8/mL)
PCV (mean ±SEM %) at baseline (0 dpi)	49.3 ± 2.6	50.3 ± 5.2	51.6 ± 7.5
% mean PCV change at day 12/PCV change at extremis‡	-2.69/-3.23	-13.27/-44.90[46]	-12.63/-59.60[115]
Time to first peak temperature (dpi)	N/A	12	8
Highest temperature increase (°C) in comparison to baseline (0 dpi)	0.68	1.80[12]	1.78[8]
Time to first detection of parasites in CSF (dpi)	N/A	12/16/16/24	8/12/16/28
Time to first detection of CSF white cell numbers > 5cells/ul (dpi)	-/-/16/24	0/8/16/28	12/16/16/28
Weight at baseline (0 dpi (Kg)	4.68 ± 0.77	4.50 ± 0.60	4.12 ± 0.60
Weight loss at extremis (Kg)	-0.6	-0.8	-1.2
Median (range) survival time (dpi)	120[b]	28 (23 - 34)	95 (57 - 115)

‡Values are from the last surviving animal in each infected cohort at extremis. The number in superscript is the day at extremis for the last serving animal in the cohort for PCV, and day of highest temperature increase in the course of infection. For CSF parasites and white cell count, the dpi for individual animals per cohort are shown and in animals where white blood cells did not reach ≥ 5cells/uL cut off, a "-" is used; b, survival time of control animals was censured data since all were euthanised at the end of the study without attaining an extremis condition.

Reduced PCV level (%) is as an indicator of anaemia. All infected animals exhibited progressive reductions in PCV during the course of infection, while uninfected animals showed insignificant fluctuations (Figure 3A). With reference to 0 dpi, the highest reductions were observed at extremis, with an average reduction of 34% in KETRI 3801 and 55% in KETRI 3928 infections at termination of the experiment at 46 and 119 dpi, respectively (see Figure 3D left panel). The rate of reduction is higher in KETRI 3801 infected cohort compared to KETRI 3928 cohort (Figure 3A). Initial drastic reduction observed around 8 - 12 dpi coincides with the time of the first peak parasitaemia. This is followed by a slight recovery, and thereafter a slow and progressive reduction. Notably, the overall magnitude of PCV reduction correlates with survival time, with the highest reduction observed at extremis in monkeys infected with KETRI 3928, which survived the longest. This is indicative of the contribution of other factors apart from PCV to shorter survival times for KETRI 3801 infected animals. In addition, a higher rate of PCV reduction is likely associated with acute infections as shown in Figure 3A.

Infected animals also had increased body temperatures as compared to controls, an indication of fever (Figure 3B). Highest average temperatures in KETRI 3801 (40.20 ℃) and KETRI 3928 (40.03 ℃) infections were observed at 12 and 8 dpi respectively, and these fall within the first peak parasitaemia. Body temperatures fluctuated throughout the course of the study period within the range of 38.30 - 38.98 ℃ (∆0.68), 38.40 - 40.20 ℃ (∆1.80) and 38.25- 40.03 ℃ (∆ 1.78) in controls, KETRI 3801 and KETRI 3928 infections respectively. This suggests greater temperature fluctuations are associated with infection. Overall, temperature increases in the monkeys were intermittent (Figure 3D middle panel) and consistent with the well known undulating fever associated with trypanosomiasis.

All infected animals registered weight loss and which increased with infection time. Total body weight includes lean mass, fluid and fat mass. A mean loss of 1.2 kg and 0.8 kg in KETRI 3928 and KETRI 3801 infections respectively were observed (Table 1, Figure 3C).

A higher rate of reduction in the KETRI 3801 infected cohort compared with the KETRI 3928 infected cohort is noted, with a loss of about 30% observed at extremis in both infections (Figure 3C and far right panel of 3D). Longitudinally, a drastic and progressive decrease in body weight begins following the first parasitaemia peak in both infection cohorts, and is followed by a brief recovery in body weight, and thereafter a steady and, drastic (for KETRI 3801 infections) or slow (for KETRI 3928 infections) decrease till extremis. With a standard feed ration and water provided *ad libitum* to all the monkeys, infection associated altered feeding and decreased feed intake, as shown in Figure S1, could in part contribute to the observed weight loss. The varying rate of loss is strain - associated, with inevitably the highest total loss at extremis (see figures 3C and 3D far right panel).

Together, PCV and body weight reduction is observed in the course of infection. Since water was provided ad libitum, and all monkeys were provided a standard feed, weight reduction can be associated with infection. Further, infection-mediated fever is initially observed at first peak parasitaemia, and remains until extremis but with some minor fluctuation. Comparatively, observations on PCV and weight loss, infection mediated fever, median survival time and risk of death indicate that KETRI 3801 is acute, while KETRI 3928 infection is chronic. A similar observation has been made in our work in the mouse model[7].

3.2.Cytokine changes with disease progression in the plasma

The outcome of an infection is the consequence of host and pathogen factors, their interactions with the host environment e.g. co-infection, and nutrition status, amongst many other factors. An important host contribution is the immune response against the infectious agent(s), and which contributes to immunopathology. Consequently, we sought to investigate immune factor alterations in the course of the two varying infection outcomes, acute and chronic, to attempt to understand which, if any, factors may have roles in modulating the course of infection. Here, parasite-induced immune-mediated pathology due to varying alterations in quantities of pro-inflammatory (IL-1β, IL-6, TNF-α, IFN-γ), anti-inflammatory (TGF-1β and IL-13) and those with both pro- and anti-inflammatory (IL-10 and IL-12) roles guided our selection. It is important to note that varying pre-infection baseline of cytokine levels due to factors such as age, sex, season and gut microbiome[26-30] among others is normal, and is responsible for differences observed at day 0 pi.

Firstly, TNF-α is a broadly influential regulator of immunity and produced by many immune cells. TNF-α plasma levels were only elevated in the monkeys infected with the chronic strain, KETRI 3928 (Figure 4A). In uninfected and monkeys infected with the acute

strain, TNF-α levels remained stable throughout the infection. A TNF-α rise was observed after 84 dpi when monkeys were confirmed to be in late-stage disease (Table 1 and Figure 5C and D).

Secondly, IL-12 was monitored, which has a major role in T cell differentiation, in particular Th1 and NK cells, as well as stimulating the production of TNF-α. At baseline, levels of IL-12 ranged between 0.8 to 1.0 ng/mL of plasma. Following infection, IL-12 levels increased to a peak by 8 dpi in both groups of infected monkeys. In the monkeys infected with KETRI 3801, the IL-12 levels at 8 dpi were three times baseline level. Thereafter, IL-12 levels declined but rose again to a second peak at 24 dpi (Figure 4B). In the monkeys infected with the chronic strain KETRI 3928, the first peak of IL-12 was twice the baseline and was observed at 8 dpi. Thereafter, IL-12 remained elevated above baseline with another peak at 60 dpi. Terminally, IL-12 levels fell to baseline. The first peak of IL-12 was significantly greater in monkeys infected with KETRI 3801 strain (Figure 4B).

IFN-γ production is also influenced by TNF-α, and is important in responses to a wide range of infections, inducing macrophage activation, and is produced by Th1 cells amongst others. A single spike of IFN-γ was observed at 8 dpi in both groups of infected monkeys (Figure 4C). No other peaks were observed thereafter until extremis. In controls, the IFN-γ levels remained steady at baseline levels throughout the duration of the study.

We next analysed soluble IL-1β levels, a cytokine involved with the inflammatory response and mainly produced by macrophages and monocytes. No notable peaks were observed in controls or monkeys infected with KETRI 3801. However, in monkeys infected with KETRI 3928, IL-1β levels in monkey 710 were significantly elevated from 16 dpi peaking at 40 dpi (Figure S2a) and showing wide variations between individuals of the cohort (wide error bars in Figure 4D). Thereafter, IL-1β levels subsided to be similar to the other animals by 64 dpi.

IL-6 is associated with microbial infections and specifically pathways mediated by Tol-like receptors. A first IL-6 peak was detected at 12 dpi in both groups of infected monkeys. In monkeys infected with the acute strain, mean IL-6 levels were significantly greater than in those infected with the chronic isolate (Figure 4E). A second IL-6 peak was evident terminally, at 95 dpi for chronic strain infections.

IL-13 is an anti-inflammation mediator, with effects on B cells causing increased IgE production. Here, plasma quantities were very low, and remained unchanged throughout the infection period (Figure S2b).

Finally, we considered IL-10, which has an anti-inflammatory function, down-regulating Th1 cytokine synthesis and antigen presentation. An increase in IL-10 levels was observed after 4 dpi in both groups of infected monkeys with those infected with the acute strain showing higher levels of the cytokine (Figure 4F). At extremis, both infected cohorts had levels that were nearly 1.5 times their baseline levels.

Taken together, the estimated effective degrees of freedom for cytokines indicated a strong evidence of highly nonlinear additive effect over time, except for TNF-α (KETRI 3801), IL-1β (KETRI 3801) and IL-6 (KETRI 3928) (Table 3). In addition, plasma cytokine levels (TNF-α, IL-1β, IFN-γ, IL-6, IL-10 and IL-12) were, as expected, significantly higher in the two groups of infected animals compared to non-infected animals at $P < 0.05$ (Table 2 and Figure 4). Notably, levels of IL-6, IL-12 and IL-10 and IFN-γ were significantly elevated in early-stage disease of both groups of infected monkeys at 8 -12 dpi suggesting that these can be considered as possible markers of early stage disease. The varying levels could also be responsible for the observed differential infection outcomes.

Table 2. Estimates from generalised additive mixed model comparing average cytokine levels (ng/ML) across two strains of *T. b. rhodesiense*.

Cytokine	Strain	Estimate	Std. Error	t-value	*P*-value
TNF-α					
	KETRI 3801	0.036	0.008	4.4	<0.001
	KETRI 3928	0.073	0.008	9.7	<0.001
IFN- γ					
	KETRI 3801	1.216	0.377	3.2	0.001
	KETRI 3928	1.223	0.313	3.9	<0.001
IL-12					
	KETRI 3801	0.850	0.105	8.1	<0.001

	KETRI 3928	0.957	0.088	10.8	<0.001
IL-1 β					
	KETRI 3801	0.134	0.010	13.4	<0.001
	KETRI 3928	0.095	0.009	10.4	<0.001
IL-6					
	KETRI 3801	0.436	0.061	7.2	<0.001
	KETRI 3928	0.121	0.051	2.4	0.018
IL-10					
	KETRI 3801	0.026	0.002	11.2	<0.001
	KETRI 3928	0.026	0.002	12.5	<0.001

317

318 Positive value means cytokine values in infected animals are higher than in controls.

319

320 **Table 3**. Estimated degrees of freedom showing trends of plasma cytokines with disease
321 progression. An E.df equal to 0 implies linear function and a greater E.df indicates
322 nonlinearity.

Cytokine	**Strain**	**E.df**	**Ref.df**	**F-value**	***P*-value**
TNF-α	KETRI 3801	0	7	0	0.999
	KETRI 3928	5.498	8	3.229	<0.001
IFN- γ	KETRI 3801	2.567	8	1.375	0.004
	KETRI 3928	4.970	8	2.548	<0.001

IL-12	KETRI 3801	3.313	8	4.821	<0.001
	KETRI 3928	6.436	8	8.660	<0.001
IL-1 β	KETRI 3801	0	8	0	0.554
	KETRI 3928	7.307	8	27.1	<0.001
IL-6	KETRI 3801	3.591	8	9.089	<0.001
	KETRI 3928	0	8	0	0.385
IL-10	KETRI 3801	3.724	8	55.17	<0.001
	KETRI 3928	7.589	8	155.7	<0.001

3.3.Cytokine changes with disease progression in the cerebrospinal fluid

To stage sleeping sickness, either the presence of parasites and/or > 5 WBC/µl in the CSF is considered an indicator of late or stage two disease (WHO, 1998). Parasites were detected in the CSF between 12 - 24 dpi and 8 - 28 dpi in KETRI 3801 and KETRI 3928 in all cohort animals, respectively (Table1, Figure 5C). Notably, early CNS invasion cannot be excluded due to the intervals of lumbar puncture for determination of parasites and WBC. Similarly, CSF WBC counts > 5 cells/µl were noted 0 – 28 dpi and 12 – 28 dpi in KETRI 3801 and KETRI 3928 infected animals, respectively. For the uninfected cohort, a WBC >0.5 cells/µl was detected in two animals at day 16 and 24 (Figure 5D, S3 and Table 1). Generally, there is a more rapid increase in CSF parasite and WBC levels in KETRI 3801 compared to KETRI 3928 infection (Figure 5C and D), and is once more indicative of more rapid parasite replication and/or invasion, progression and severity of late-stage disease in KETRI 3801 infections as compared to KETRI 3928 infections.

In the CSF, the levels of six cytokines were extremely low, except for IL-12 (in monkey 715 and 709, Figure S2b), TGF-1β and SB100β. A limitation here is that marker levels are low and often at undetectable levels (Tarrant, 2010). TGF-1β has multiple roles in

inflammation, mainly acting to suppress B cell and macrophage activity as well as promoting differentiation of CD4 T cells. A variable TGF-1β response was observed in the monkey cohort. In monkeys infected with KETRI 3801, two animals, 708 and 704 showed an increasing trend with reference to baseline; a peak at 4 dpi and 24 dpi (Figure 5 and S2b). In monkeys infected with KETRI 3928, the levels in monkey 699 were elevated throughout the infection (Figure S2b) with variable response in the remaining two monkeys.

S100β is secreted by mature astrocytes and is a marker of CNS injury and blood brain barrier permeability. Wide variations in S100β levels were observed. In KETRI 3801 infected monkeys, two individuals 704 and 708 showed an increase during infection, whereas in KETRI 3928 infected monkeys, a variable response with no obvious trend was observed (Figure S2b).

In summary, the majority of CSF assayed immune factors remain unchanged throughout the course of infections except for IL-12 (in two animals), TGF-1β and SB100β. Further, higher CSF parasite and WBC counts are observed earlier in second stage disease for KETRI 3801(acute) as compared to KETRI 3928 (chronic) infection.

4. Discussion

African trypanosomes have multiple and elaborate strategies to evade mammalian host defenses permitting long survival and an increase in their transmission window. Among these is antigenic variation, a systematic change to their dense surface coat, variable surface glycoprotein (VSG), to avoid detection and clearance by host antibodies. The VSG is also a protective layer for antigenic invariant surface molecules, including invariant surface glycoprotein 65 (ISG65) that limits complement mediated killing[31-33] and ISG75 that binds Fc regions of immunoglobulins[34]. Further, surface hydrodynamic flow on motile parasites drag antibody - surface proteins complexes to flagellar pocket[35], where the complexes are internalised, antibodies degraded while the surface proteins including VSGs recycled back to the surface[36,37]. This limits antibody mediated clearance, and with membrane trafficking upregulated in blood stage parasites[37], it is a considerable defensive protection. Additional resistance strategy is in operation on human infective trypanosomes, where they express serum resistance associated (SRA) protein and *T. b. gambiense*-specific glycoprotein (TgsGP) that neutralise human serum trypanolytic factor (TLF)[38,39]. While these defense strategies are clear, our knowledge on trypanosome directed suppression and/or alteration of host immune response to favour their survival is still limited, and differential immune responses, as determined by species and strain of trypanosomes and hosts, and mode of

infection[40] determine infection outcome, despite the common presence of these immune evasion systems. Using the NHP model of HAT, we interrogated the evolution of clinical and immune responses of vervet monkeys infected with two strains of *T. b. rhodesiense* responsible for varying infection outcomes, acute (KETRI 3801) and chronic (KETRI 3928) sleeping sickness.

The tsetse-mediated infection by a single blood meal bite[12] mimics natural infection, and was accompanied by the presence of a trypanosomal chancre at the sites of the bite in some infections. Chancre results from a localised inflammatory response to the inoculated parasites[41,42], tsetse salivary components[43,44] and possibly laceration caused by probing for hemorrhagic pool feeding. It is the host first attempt to prevent and contain initial parasite colonisation. But, a chancre is not observed in all bites, and is suggested to vary depending on both the infecting species and host[45,46], and the molecular basis underpinning this remains unknown. Thereafter, we observed higher primary peak parasitaemia, replication rate and parasitaemia in strain KETRI 3801 compared to KETRI 3928 (see figure 2A). A similar trend is observed in the mouse model[7], where differences in strain dependent factors on replication (proliferation and differentiation) and host-mediated clearance could play a role. In addition, the lower KETRI 3928 parasitaemia is a characteristic associated with chronic trypanosome infections as previously observed by Turner et al.[47]. Possibly, KETRI 3928 maintains sublethal levels by balancing host clearance and differentiation into non-dividing stumpy forms, and proliferation, without having adverse effects on the hosts and hence longer host survival and extended transmission window. Observations by Murray and Morrison[48] that higher parasitaemia is associated with a higher degree of pathogenesis in part explain the adverse pathologies observed in acute infection.

We observed acute (KETRI 3801 infection) and chronic (KETRI 3928 infection) infection outcomes as inferred from the impact of infection (anaemia, loss of body weight and likelihood of survival) and survival (Figures 1, 2 and 3). The outcome is most likely strain dependent: First, short (28 days) and long (95 days) (Figure 1B, 2B and Table 1) survival is observed, respectively, in KETRI 3801 and KETRI 3928 infections of both vervet monkeys here, and in mice[7]. In addition, the risk of death is three-fold higher in KETRI 3801 infections compared to KETRI 3928 infection (Figure 2C). Second, hosts within each cohort consistently exhibit a similar outcome, indicative of strain-associated factors. If this were not the case, we would expect significantly more stochastic outcomes in the measured parameters between the members of a cohort. We can therefore suggest that any immunopathology that differentially manifests between the KETRI 3801 and 3928 infected cohorts are a consequence of strain-directed differential immune responses. This suggests

411 that immune cells and factors (e.g. cytokines, chemokine, growth factors and signalling
412 molecules), their quantities, dynamics and/or locality determine the evolution of immune
413 response and immunopathology, and hence the final outcome.

414 Anaemia is a common symptom in African trypanosome infections, and due to
415 immunopathology leading to erythrophagocytosis and/or reduced erythropoiesis.
416 Principally, persistent initial type 1 pro-inflammatory responses result in acute anaemia. A
417 subsequent IL-10 mediated resolution into type 2 anti-inflammatory response manifests as
418 chronic anaemia. Here, we can infer that strain-directed immunomodulation could be
419 responsible for the varying degree of anaemia severity (see Figure 3A), with pro-
420 inflammatory cytokines IL-1β, IL-6, IFN-γ and TNF-α implicated. For example, as in humans,
421 rhesus macaques and the murine model, IL-6 which is 6 fold higher in KETRI 3801 than
422 KETRI 3928 infections at 12 pi (Figure 4E), in a reversible and dose-dependent fashion[49-51]
423 could direct reduction of serum iron[51], consequently suppressing erythropoiesis. Similarly,
424 IFN-γ (Figure 4C) possibly contribute by inhibiting erythroblast proliferation and
425 differentiation, suppressing erythropoiesis as observed elsewhere[52,53]. On the other hand,
426 IL-12, which remains moderately higher throughout in KETRI 3928 infection but decreases
427 towards extremis (Figure 4B), and is a direct dose-dependent stimulator of
428 erythropoiesis[54]and protective against anaemia[55], could permit a gradual loss of protection,
429 and hence the resulting chronic anaemia. In sum, we infer that strain-directed IL-6, IFN-γ
430 and IL-12 levels could explain the acute and chronic anaemia observed in the cohorts.

431 Food and water were provided *ad libitum*, yet weight loss was observed; higher in acute
432 as compared to chronic infections (Figure 3C and D, and Table 1). This loss is most likely
433 infection-induced, and variation strain dependent. Two reasons could account for this. First,
434 an infection-induced hypohagia (Figure S1), a feature that has also been observed in murine
435 models of African trypanosomiasis[7,56] and worm infection[57] and a loss of appetite in humans.
436 The hypophagia could be a consequence of a satiety signal from feed control centres of the
437 brain mediated directly or indirectly by immune factors and/or hormones like leptin[58,59].
438 Second, immune-directed reduction of components of body weight i.e. fluid, lean and fat
439 mass, as recently observed in the murine model of African trypanosomiasis[60,61] could be at
440 play. Inference from *in vitro* and mouse model studies, hypophagia and immune-mediated
441 reduction of lean and fat mass can explain the weight loss in our vervet monkey model of
442 HAT.

443 Fever is a part of acute phase responses with a protective role[62]; the febrile temperature
444 acts as stressor, harming replicating pathogens[63], increasing their susceptibility to

445 destruction and stimulating both innate and adaptive immune response[64]. This protective
446 role could be responsible for reductions in parasitaemia preceded by peak febrile
447 temperatures observed here. In addition, characteristic intermittent infection-associated
448 fevers point to the hosts ability to control intensity and timing, indicative of a host response
449 to infection rather than a direct pathogen-driven process. The central endogenous pyrogenic
450 actor is IL-6, augmented with other mediators such as IL-1, TNF-α, cyclooxygenase 2
451 (COX2) and prostaglandin E_2 (PGE2)[65-68]. Also necessary are pathogen factors that act as
452 exogenous pyrogens, whose detection by resident innate immune cells elicit IL-1 and IL-6
453 production, and also activate PGE2 synthesis[69]. Trypanosome glycosylphosphatidylinositol
454 (GPI) is a prime candidate exogenous pyrogen, having been shown by others[70-72] to elicit
455 production of innate cytokines, including IL-6. The higher levels of IL-6 in infected cohorts
456 (Table 2; Figure 4E) could explain the increase to core body temperature, while differences
457 in febrile responses between acute and chronic infections could be due to strain-related
458 varying levels of fever mediators. For example a differential IL-6 activation of COX2 in
459 endothelial cells in hypothalamic microvessels[73,74] (consequently cerebral PGE2 levels) in a
460 dose-dependent fashion. It is plausible that pyrogenic cytokines and pathogen factors
461 contribute to fever in our NHP HAT model.

462 Crucial in determining infection outcomes are immune factors that link innate and
463 adaptive immune responses, as they regulate the protective and deleterious roles of pro-
464 inflammation. Here, key crossroad mediator candidates are IL-12 and IL-10, and their
465 downstream actors. For example, pro- and anti-inflammatory IL-6[75] whose secretion is
466 influenced by IL-12[76-78] could be important in resolution of immune response and outcomes
467 observed here. Elevated IL-6 levels as in acute KETRI 3801 infection, are associated with
468 highly virulent strains in other infections[79,80], and is predictive of disease severity as reported
469 in bovine trypanosomiasis[81]. The IL-6 levels would differentially modulate pro-inflammation
470 by IFN-γ whose levels are the same in both cohorts. Similarly, IL-10 promotes pathogen
471 eliminating pro-inflammation assaults but also suppresses or attenuates hyper-inflammation
472 to ameliorate immune-mediated tissue damage. In Figure 4F, we observed steady
473 upregulation of IL-10 as in Ngotho et al.[82] followed by maintenance at higher levels. The
474 upregulation by day 4 pi (as with IL-6, IL-12 and IFN-γ; Figure 4) could indicate early efforts
475 to control hyper-inflammation and potential tissue damage, while maintaining protective
476 inflammation. The slow progressive increase could permit rapid activation of innate and
477 adaptive response for effective pathogen elimination. Thereafter, the subsequent steady
478 levels could be immunosuppressive, favouring host tolerance and long survival of pathogen
479 in chronic infections. Similar responses have been proposed in various infections including

Toxoplasma gondii[83], leishmania[84] and viruses[85], and could explain the lower but steady KETRI 3928 parasitaemia. Therefore, differential expression of IL-12 and IL-10 and their downstream mediators e.g. IL-6, could play a pivotal role in crosstalk between innate and adaptive immunity, indicative of varying immunomodulation and immunopathologies, which manifest as acute and chronic outcomes.

Positive detection of parasites in blood is accompanied by staging that involves a painful and invasive lumbar puncture to determine CSF parasites and/or WBC. Here, while days of CNS invasion (between week 2 and 3; table 1) were not different, we observed a higher CSF parasitaemia early in KETRI 3801 (acute) as compared to KETRI 3928 (chronic) infection (Figure 5C). CSF is a unique and hostile microenvironment[86,87] and reasons for variation in parasitaemia could be; i) retention of the replication rates in BSF and CSF forms, and is corroborated by reports of similarity in impact of these two forms in mice[88]; ii) a varying survival ability in CSF; or (iii) varying bidirectional transmigration abilities, if in part, invasion is influenced by BSF levels and pathogen directed immunomodulation as suggested by others[89,90]. In addition, an increase in WBC after parasite CNS invasion and with disease progression suggest parasite-induced recruitment as observed by Frevert and colleagues[91] in the murine model. Considering individual infected animals of each cohort and their survival, a combination of other factors together with CSF parasitaemia are implicated in late-stage fatality. Our preliminary observations using these strains in a vervet monkey model of HAT could be valuable in interrogating mechanism of invasion and associated impairments, timing and clarity on evolution of early into late-stage disease, since neurological characteristics have been observed in early stage patients[92].

In summary, we show the immune and clinical impacts for two *Tbr* strains KETRI 3801 and KETRI 3928, responsible for acute and chronic infection outcome respectively. We infer this from anaemic states, weight loss, risk of death and survival time. Here, we suggest a strain-directed and host-dependent immunomodulation as the basis of the different infection outcomes. This will need further qualification by establishing individual roles of the immune factors and integrating this to their complex network. Insight gathered will be important in understanding HAT progression that can be helpful in identifying staging biomarkers and improve clinical management of cases. In the context of vector transmitted pathogens, maladaptation to strains causing acute infections marked by short host survival and hence narrow transmission window could be suggested.

REFERENCES

1. Simarro, P. P. et al. Human African trypanosomiasis in non-endemic countries (2000–2010). *J Travel Med* **19**, 44-53 (2012).
2. Franco, J. R. et al. Human African trypanosomiasis cases diagnosed in non-endemic countries (2011–2020). *PLoS Negl Trop Dis* **16**, e0010885 (2022).
3. WHO. (2022). Trypanosomiasis, human African (sleeping sickness). https://www.who.int/news-room/fact-sheets/detail/trypanosomiasis-human-african-(sleeping-sickness
4. Franco, J. R. et al. Monitoring the elimination of human African trypanosomiasis at continental and country level: Update to 2018. *PLoS Negl Trop Dis* **14**, e0008261 (2020).
5. Shah, V. V., Patel, V. M. & Vyas, P. Human African Trypanosomiasis–A rare case report from India. *Indian J Med Microbiol* **40**, 169-171(2022).
6. Ndung'u, K. et al. Differential virulence of *Trypanosoma brucei rhodesiense* isolates does not influence the outcome of treatment with anti-trypanosomal drugs in the mouse model. *PLoS One* **15**, e0229060 (2020).
7. Limo, W. K. et al. Mouse experiments demonstrate differential pathogenicity and virulence of *Trypanosoma brucei rhodesiense* strains. *Exp Parasitol* **228**, 108135 (2021).
8. MacLean, L. et al. Severity of human African trypanosomiasis in East Africa is associated with geographic location, parasite genotype, and host inflammatory cytokine response profile. *Infec Immun* **72**, 7040-7044 (2004).
9. Kato, C. D., Matovu, E., Mugasa, C. M., Nanteza, A., & Alibu, V. P. The role of cytokines in the pathogenesis and staging of T*rypanosoma brucei rhodesiense* sleeping sickness. *Allergy, Asthma Clin Immunol 1***2**, 1-10 (2016).

10. Kato, C. D., Alibu, V. P., Nanteza, A., Mugasa, C. M., & Matovu, E. Interleukin (IL)-6 and IL-10 are up regulated in late stage *Trypanosoma brucei rhodesiense* sleeping sickness. *PLoS Negl Trop Dis* **9**, e0003835 (2015).

11. Kamoto, K. et al. Plasma cytokines quantification among *Trypanosoma brucei rhodesiense* sleeping sickness cases and controls in Rumphi, Malawi. *Malawi Med J* **33**, 230-235 (2021).

12. Thuita, J. K. et al. *Trypanosoma brucei rhodesiense* transmitted by a single tsetse fly bite in vervet monkeys as a model of human African trypanosomiasis. *PLoS Negl Trop Dis* **2**, e238 (2008).

13. MacLean, L., Odiit, M. & Sternberg, J. M. Nitric oxide and cytokine synthesis in human African trypanosomiasis. *J Infect Dis* **184**, 1086-1090 (2001).

14. Namangala, B., Noël, W., De Baetselier, P., Brys, L. & Beschin, A. Relative contribution of interferon-gamma and interleukin-10 to resistance to murine African trypanosomiasis. J Infect Dis. **183**, 1794 -1800 (2001).

15. Sternberg, J. M. et al. Meningoencephalitic African trypanosomiasis: Brain IL-10 and IL-6 are associated with protection from neuro-inflammatory pathology. *J Neuroimmunol*, **167**, 81-89 (2005).

16. Rothermundt M., Peters M., Prehn J. H. & Arolt V. S100B in brain damage and neurodegeneration. *Microsc Res Tech.* **60**, 614–632 (2003).

17. Marchi, N. et al. Peripheral markers of blood-brain barrier damage. *Clin Chim Acta* **342**, 1–12 (2004).

18. Bloomfield S. M., McKinney, J., Smith, L. & Brisman, J. Reliability of S100B in predicting severity of central nervous system injury. *Neurocrit Care* **6**,121–138 (2007).

19. Laudenslager, M. L., Fairbanks L. A. & Jorgensen, M. J. Plasma cytokine levels: Relationship to early maternal interactions in socially reared vervet monkeys (*Cercopithecus aethiops sabaeus*). *Brain Behav Immun* **20**, e34-e35 (2006).

20. Zhang, W. et al. *Schistosoma mansoni* antigen Sm-p80: prophylactic efficacy using TLR4 agonist vaccine adjuvant glucopyranosyl lipid A-Alum in murine and non-human primate models. *J Investig Med* **66**, 1124 - 1132 (2018).

21. Willis, E. L., Eberle, R., Wolf, R. F., White, G. L. & McFarlane, D. Effects of chronic viral infection on lymphocyte populations in middle-aged baboons (*Papio anubis*). *Comp Med* **71**, 177- 187 (2021).

22. Wood, S. N. Generalized additive models: an introduction with R. *Chapman and Hall/CRC* (2017).

23. Wood, S. N. Stable and efficient multiple smoothing parameter estimation for generalized additive models. *J Amer Stat Asso* **99**, 673-686 (2004).

24. Kirkwood, B. R. & Sterne, J. A. Essential medical statistics. *John Wiley & Sons* (2010).

25. R Core. Team R: A language and environment for statistical computing. R Foundation for Statistical Computing, Vienna, Austria. URL https://www.R-project.org/ (2019).

26. Mascarucci, P. et al. Age-related changes in cytokine production by leukocytes in rhesus monkeys. *Aging (Milano)* **13**,85-94 (2001).

27. McFarlane, D., Wolf, R. F., McDaniel, K. A. & White, G. L. Age-associated alteration in innate immune response in captive baboons. *J Gerontol A Bill Sci Med Sci* **66**, 1309 - 1317 (2011).

28. McFarlane, D., Wolf, R. F., McDaniel, K. A. & White, G. L. The effect of season on inflammatory response in captive baboons. *J Med Primatol* **41**, 341 - 348 (2012).

29. Schirmer, M. et al. Linking the human gut microbiome to inflammatory cytokine production capacity. *Cell* **167**, 1125-1136.e8 (2016).

30. Stone, L. H. et al. Serum cytokine profiles in healthy nonhuman primates are blunted by sedation and demonstrate sexual dimorphism as detected by a validate multiplex immunoassay. *Sci Rep* **11**, 2340 (2021).

31. MacLeod, O. J. S. et al. Invariant surface glycoprotein 65 of Trypanosoma brucei is a complement C3 receptor. *Nat Commun* **13**, 5085 (2022).

32. Lorentzen, J. et al. *Trypanosoma brucei* invariant surface pg65 inhibits the alternative pathway of complement by accelerating C3b degradation. *J Immunol* **211**, 862-873 (2023).

33. Sülzen, H. et al. Cryo-EM structures of *Trypanosoma brucei gambiense* ISG65 with human complement C3 and Cb3 and their roles in alternative pathway restriction. *Nat Commun* **14**, 2403 (2023).

34. Mikkelsen, J. H. et al. *Trypanosoma brucei* invariant surface glycoprotein 75 is an immunoglobulin Fc receptor inhibiting complement activation and antibody-mediated cellular phagocytosis. *J Immunol* **212**,1334-1344 (2024).

35. Engstler, M. et al.Hydrodynamic flow-mediated protein sorting on the cell surface of trypanosomes. *Cell* **131**, 505-515 (2007) .

609 36. Engstler, M. et al. Kinetics of endocytosis and recycling of GPI-anchored variant surface
610 glycoprotein in *Trypanosoma brucei. J Cell Sci* **117**, 1105 - 1115 (2004) .

611 37. Koumandou, V. L., Natesan, S. K. A., Sergeenko, T. & Field, M. C. The trypanosome
612 transcriptome is remodelled during differentiation but displays limited responsiveness
613 within life stages. *BMC Genomics*. **9**, 298 (2008).

614 38. Xong, H.V. et al. A VSG expression site-associated gene confers resistance to human
615 serum in *Trypanosoma rhodesiense*. *Cell* **95**, 839–846 (1998).

616 39. Capewell, P. et al. The TgsGP is essential for resistance to human serum in
617 *Trypanosoma brucei gambiense*. PLoS Pathog **9**,e1003686 (2013).

618 40. Wei, G., Bull, H., Zhou, X. & Tabel, H. Intradermal infections of mice by low numbers of
619 African trypanosomes are controlled by innate resistance but enhance susceptibility to
620 reinfection. J Infect Dis. **203**, 418-429 (2011).

621 41. McGovern, T. W. et al. Cutaneous manifestations of African trypanosomiasis. *Arch*
622 *Dermatol* **131**, 1178-1182 (1995).

623 42. Sekhar, G. N., Watson, C. P., Fidanboylu, M., Sanderson, L. & Thomas, S. A. Delivery
624 of antihuman African trypanosomiasis drugs across the blood–brain and blood–CSF
625 barriers. *Adv Pharmacol* **71**, 245-275 (2014).

626 43. Caljon, G. et al. Tsetse fly saliva accelerates the onset of *Trypanosoma brucei* infection
627 in a mouse model associated with a reduced host inflammatory response. *Infect Immun*
628 **74**, 6324-6330 (2006).

629 44. Alfituri, O. A. et al. To the skin and beyond: The immune response to African
630 trypanosomes as they enter and exit the vertebrate host. *Front Immunol* **11**, 526809
631 (2020).

632 45. Urech, K., Neumayr, A. & Blum, J. Sleeping sickness in travellers-do they really sleep?
633 *PLoS Negl Tropic Dis* **5**, e1358 (2011).

634 46. Crilly, N. P. & Mugnier, M. R. Thinking outside the blood: Perspectives on tissue-resident
635 *Trypanosoma brucei*. *PLoS Pathog* **17***,* e1009866 (2021).

636 47. Turner, C. M. R., Aslam, N. & Dye, C. Replication, differentiation, growth and the
637 virulence of *Trypanosoma brucei* infections. *Parasitol* **111**, 289 - 300 (1995).

638 48. Murray, M., & Morrison, W. (1978). Parasitemia and host susceptibility to African
639 trypanosomiasis. Pathogenicity of trypanosomes: proceedings of a workshop held at
640 Nairobi, Kenya, 20-23 November 1978. IDRC-132e.

641 49. van Gameren, M. M. et al. Effects of recombinant human interleukin-6 in cancer patients:
642 a phase I-II study. *Clinical Trial Blood* **84**, 1434-1441 (1994).

643 50. Winton, E. F. et al. Effect of recombinant human interleukin-6 (rhIL-6) and rhIL-3 on
644 hematopoietic regeneration as demonstrated in a nonhuman primate chemotherapy
645 model. Blood **84**, 65-73 (1994).

646 51. Neves, J. V. et al. A role for hepcidin in the anemia caused by Trypanosoma brucei
647 infection. *Haematologica* **106**, 806 (2021).

648 52. Felli, N. et al. Multiple members of the TNF superfamily contribute to IFN-γ-mediated
649 inhibition of erythropoiesis. *J Immunol* **175**, 1464-1472 (2005).

650 53. Cnops, J. et al. NK-, NKT-and CD8-derived IFNγ drives myeloid cell activation and
651 erythrophagocytosis, resulting in trypanosomosis-associated acute anemia. *PLoS*
652 *Pathog* **11**, e1004964 (2015).

653 54. Dybedal, I., Larsen, S. & Jacobsen, S. IL-12 directly enhances in vitro murine
654 erythropoiesis in combination with IL-4 and stem cell factor. *J Immunol* **154**, 4950-4955
655 (1995).

656 55. Zhang, L. et al. Polymorphisms in genes of interleukin 12 and its receptors and their
657 gene association with protection against severe malarial anaemia in children in western
658 Kenya. *Malar J* B, 87 (2010).

659 56. Trindade, S. et al. *Trypanosoma brucei* parasites occupy and functionally adapt to the
660 adipose tissue in mice. *Cell Host Microbe*, **19** 837-848 (2016).

661 57. Worthington, J. J., Samuelson, L. C., Grencis, R. K. & McLaughlin, J. T. Adaptive
662 immunity alters distinct host feeding pathways during nematode induced inflammation,
663 a novel mechanism in parasite expulsion. *PLoS Pathog* **9** e1003122 (2013).

664 58. Ahima, R. S. & Antwi, D. A. Brain regulation of appetite and satiety. *Endocrinol Metab*
665 *Clin North Am* **37,** 811-823 (2008).

666 59. Maurya, R., Bhattacharya, P., Dey, R. & Nakhasi, H. L. Leptin functions in infectious
667 diseases. *Front Immunol*, **9,** 374648.

668 60. Machado, H., Hofer, P., Zechner, R., Smith, T. K. & Figueiredo, L. M. Adipocyte lipolysis
669 protects mice against *Trypanosoma brucei* infection. *Nature Microbiol* **8,** 2020-2032
670 (2023).

61. Redford, S. E., Varanasi, S. K., Sanchez, K. K., Thorup, N. R. & Ayres, J. S. CD4+ T cells regulate sickness-induced anorexia and fat wasting during a chronic parasitic infection. *Cell Rep* **42,** 112814 (2023).

62. LeGrand, E. K. & Day, J. D. Self-harm to preferentially harm the pathogens within: non-specific stressors in innate immunity. *Proc Biol Sci* **283,** 20160266 (2016).

63. LeGrand, E. K. & Alcock, J. Turning up the heat: immune brinksmanship in the acute-phase response. *Q Rev Biol* **87,** 3-18 (2012).

64. Evans, S. S., Repasky, E. A. & Fisher, D. T. Fever and the thermal regulation of immunity: the immune system feels the heat. *Nature Rev Immunol*, **15**, 335-349 (2015).

65. Sundgren-Andersson, A. K., Östlund, P. & Bartfai, T. IL-6 is essential in TNF-α-induced fever. *Am J Physiol* **275** R2028-R2034 (1998).

66. Cartmell, T., Poole, S., Turnbull, A., Rothwell, N. & Luheshi, G. Circulating interleukin-6 mediates the febrile response to localised inflammation in rats. *J Physiol* **526**, 653-661 (2000).

67. Li, S., Goorha, S., Ballou, L. R. & Blatteis, C. M. Intracerebroventricular interleukin-6, macrophage inflammatory protein-1β and IL-18: pyrogenic and PGE2-mediated? *Brain Res* **992**, 76-84 (2003).

68. Nilsberth, C., et al. The role of interleukin-6 in lipopolysaccharide-induced fever by mechanisms independent of prostaglandin E2. *Endocrinol* **150**, 1850-1860 (2009).

69. Martínez-Colón, G. J., & Moore, B. B. Prostaglandin E2 as a regulator of immunity to pathogens. *Pharmacol & Ther* **185**, 135-146 (2018).

70. Tachado, S. D. & Schofield, L. Glycosylphosphatidylinositol toxin of Trypanosoma bruce regulates IL-1 alpha and TNF-alpha expression in macrophages by protein tyrosine kinase mediated signal transduction. *Biochem Biophys Res Commun* **205**, 984-991 (1994).

71. Magez, S., et al.The gylycosyl-inositol-phosphate and dimyristoylglycerol moieties of the glycosylphosphatidylinositol anchor of the trypanosome variant-specific surface glycoprotein are distinct macrophage-activating factors. *J Immunol.* **160**,1949-1956 (1998).

72. Stijlemans, B., Baral, T. N., Guilliams, M., Brys, L., Korf, J., Drennan, M., Van Den Abeele, J., De Baetselier, P., Magez, S. (2007) A glycosylphosphatidylinositol-based

treatment alleviates trypanosomiasis-associated immunopathology. J Immunol. 179(6),4003-4014.

73. Yamagata, K., et al. Coexpression of microsomal-type prostaglandin E synthase with cyclooxygenase-2 in brain endothelial cells of rats during endotoxin-induced fever. *J Neurosci* **21**, 2669-2677 (2001).

74. Rummel, C., Sachot, C., Poole, S. & Luheshi, G. N. Circulating interleukin-6 induces fever through a STAT3-linked activation of COX-2 in the brain. *Am J Physiol Regul Integr Comp Physiol* **291**, R1316-R1326 (2006).

75. Scheller, J., Chalaris, A., Schmidt-Arras, D. & Rose-John, S. The pro-and anti-inflammatory properties of the cytokine interleukin-6. *Biochim Biophys Acta* **1813**, 878-888 (2011).

76. Cahill, C. M. & Rogers, J. T. Interleukin (IL) 1β induction of IL-6 is mediated by a novel phosphatidylinositol 3-kinase-dependent AKT/IκB kinase α pathway targeting activator protein-1. *J Biol Chem*, **283**, 25900-25912 (2008).

77. Wu, H., Liu, G. & Shi, M. Interferon gamma in African trypanosome infections: friends or foes? *Front Immunol* ***8***, 289078 (2017).

78. Kak, G., Raza, M. & Tiwari, B. K. Interferon-gamma (IFN-γ): Exploring its implications in infectious diseases. *Biomol Concepts*, **9**, 64-79 (2018).

79. Ng, L. F. et al. IL-1β, IL-6, and RANTES as biomarkers of Chikungunya severity. *PLoS One* **4**, e4261 (2009).

80. Velazquez-Salinas, L., Pauszek, S. J., Arzt, J. & Rodriguez, L. L. Increased virulence of an epidemic strain of vesicular stomatitis virus is associated with interference of the innate response in pigs. *Front Microbiol* **9**, 396917 (2018).

81. Kuriakose, S. M., Singh, R. & Uzonna, J. E. (2016). Host intracellular signalling events and pro-inflammatory cytokine production in African trypanosomiasis. *Front Immunol* **7**, 182445.

82. Ngotho, M. et al. IL-10 is up regulated in early and transitional stages in vervet monkeys experimentally infected with *Trypanosoma brucei rhodesiense*. *Parasitol Inter* **55**, 243-248 (2006).

83. Wilson, E. H., Wille-Reece, U., Dzierszinski, F. & Hunter, C. A. A critical role for IL-10 in limiting inflammation during toxoplasmic encephalitis. *J Neuroimmunol* **165**, 63-74 (2005).

84. Anderson, C. F. et al. IL-10 and TGF-beta control the establishment of persistent and transmissible infections produced by *Leishmania tropica* in C57BL/6 mice. *J Immunol* ***180***,4090-4097 (2008).

85. Ribeiro, S. P. et al. IL-10 driven memory T cell survival and Tfh differentiation promote HIV persistence. *BioRxiv*, **26,** 432955 (2021)..

86. Pentreath, V. Cytokines and the blood-brain barrier in human and experimental African trypanosomiasis. In progress in human African trypanosomiasis, sleeping sickness. *Springer* 105-117 (1999).

87. Wolburg, H. et al. Late stage infection in sleeping sickness. PLoS ONE. **7**, e34304 (2012).

88. Ndung'u, K. et al. Pathogenicity of bloodstream and cerebrospinal fluid forms of *Trypanosoma brucei rhodesiense* in Swiss white mice. *African J Health Sci* **15**, 34-41 (2008).

89. Mogk, S. et al. Cyclical appearance of African trypanosomes in the cerebrospinal fluid: new insights in how trypanosomes enter the CNS. *PLoS One*, **9**, e91372 (2014)..

90. Laperchia, C. et al. Trypanosoma brucei invasion and T-cell infiltration of the brain parenchyma in experimental sleeping sickness: timing and correlation with functional changes. *PLoS Negl Trop Dis* **10**, e0005242 (2016)..

91. Frevert, U. et al. Movila, A., Nikolskaia, O. V., Raper, J., Mackey, Z. B., Abdulla, M., McKerrow, J., & Grab, D. J. Early invasion of brain parenchyma by African trypanosomes. *PLoS One* **7**, e43913 (2012).

92. MacLean, L. M., Odiit, M., Chisi, J. E., Kennedy, P. G. & Sternberg, J. M. Focus–specific clinical profiles in human African trypanosomiasis caused by *Trypanosoma brucei rhodesiense*. *PLoS Negl Trop Dis* **4**, e906 (2010).

Conflicts of interest

The authors of this paper declare no conflict of interest.

Authorship contribution statement

V.O.A., M. C.F., D.M. and E.M. conceived and designed the experiment. J.C., J.K.T.,O.J. and V.O.A. did the experiments. V.O.A., M. C.F., D.M. and J.K. T. interpreted the data. O.B.O. undertook statistical analysis and interpretation of the data. All authors except O.J. undertook the drafting of the manuscript.

Acknowledgement

The authors would like to thank the Institute Director of Biotechnology Research Institute of Kenya Agricultural and Livestock Research Organization (BioRI-KARLO) and staff for facilitation and providing technical expertise. Gratitude to The International Centre of Insect Physiology and Ecology (*icipe*) for grant administration.

Funding

This work was supported by the Wellcome Trust [grant number 101166/Z/13/Z] to VOA.

A

Strain ID	Year of isolation	Isolate type	Region of isolation	Lab derivative ID	Derivative type	Passages
KETRI 3199	1989	Pleiomorphic	Busia, Kenya	KETRI 3801	Clone	1
KETRI 3928*	2003	Clone	Tororo, Uganda	KETRI 3928	Clone	2

B

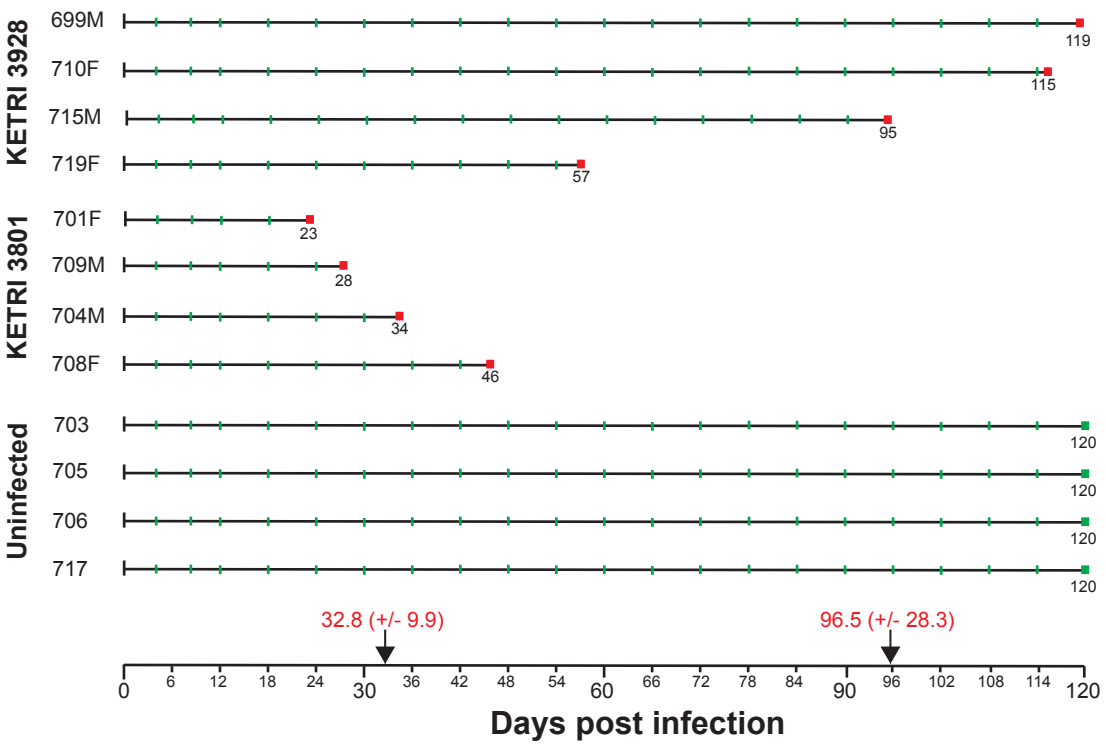

Figure 1: Strain biodata and sampling regime. A. Biological and historical data of *T. b. rhodesiense* strains used in the study. **B.** Eight *C. pygerythrus* had been infected with the indicated strains of *T. b. rhodesiense*, while four were uninfected. Blood and CFS samples taken as indicated by the green tick marks. Animals were sacrificed at the times shown by red boxes due to emergence of clear late stage symptoms. The mean survival time (plus the SD) are shown for the infected cohorts. F = female, M = male. These samples formed the resource for the study. *A cloned strain donated to KALRO-BioRI laboratory by National Livestock Resource Research Institute (NaLIRRI) of Uganda.

A. Parasitaemia

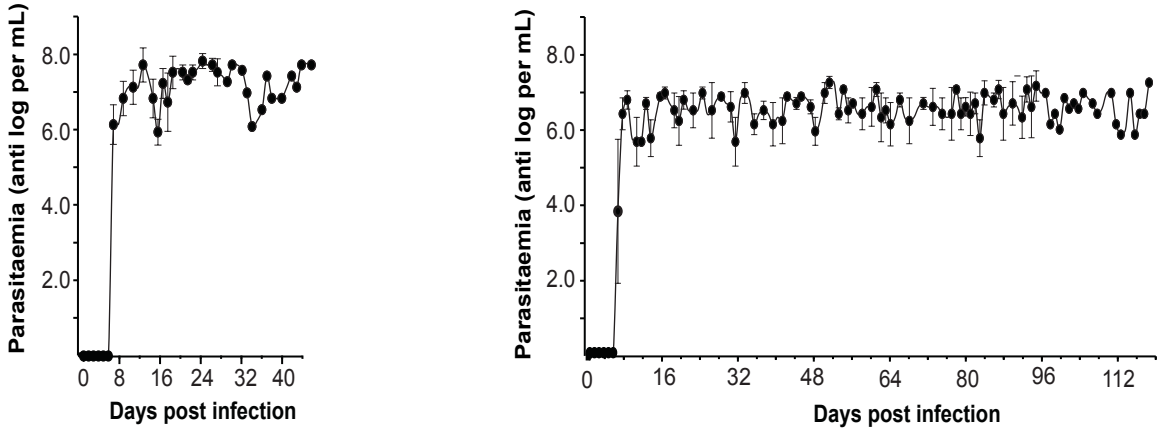

B. Survival curves

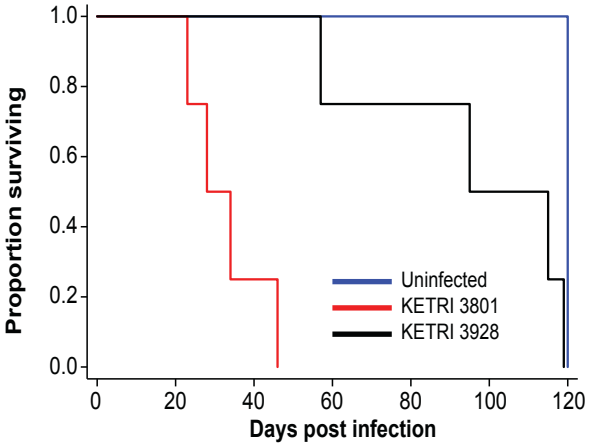

C. Estimated risk of dying

Strain	Hazard ratio (95% CI)	p-value
Control		
KETRI 3801	2.48 (1.42 - 4.3)	0.001
KETRI 3928	0.66 (0.42 - 1.0)	0.070

Figure 2.0. Parasitaemia and survival of vervet monkey infected with different strains of *T. b. rhodesiense.* A. The two strains KETRI 3801 and KETRI 3928 exhibit first peak parasiatemia above antilog 7.0 per mL. This is follwed by subbsquent peaks, with a much smaller range of 6 - 8 observed in KETRI 3928 infection. **B**. Kaplan-Meier (survival) curves for uninfected, KETRI 3801 infected and KETRI 3928 infected monkeys show that KETRI 3801 is the most virulent strain compared to KETRI 3928. Survival curves differed significantly across the strains (Log-rank test $p<0.001$). **C**. Estimated risk of dying using cox proportional hazard model is higher in KETRI 3801 infection as compared to KETRI 3928.

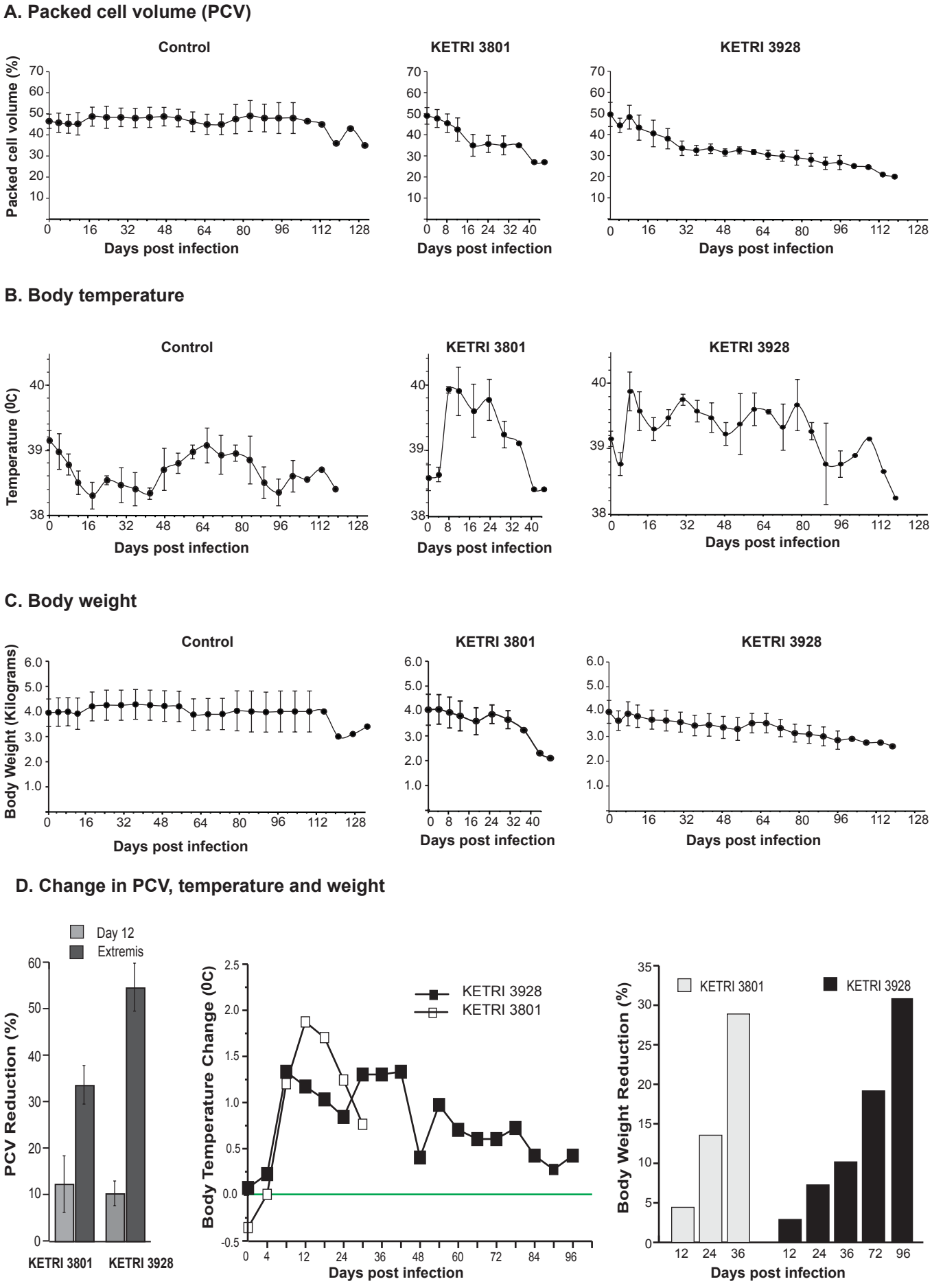

Figure 3.0. Impact of *T. b. rhodesiense* strains on vervet monkey. Effect on **A**. packed cell volume (PCV), **B**. body temperature and **C**. body weight of vervet monkeys infected with two strains of *T. b. rhodesiense* KETRI 3801 and 3928 that cause acute ad chronic infections respectively. Percent PCV and weight reductions at specific post infection time points are shown in **D** far left and far right panels. Change in temperature at corresponding time points of infected animals compared to uninfected are shown in middle panel, and is indicative of fever.

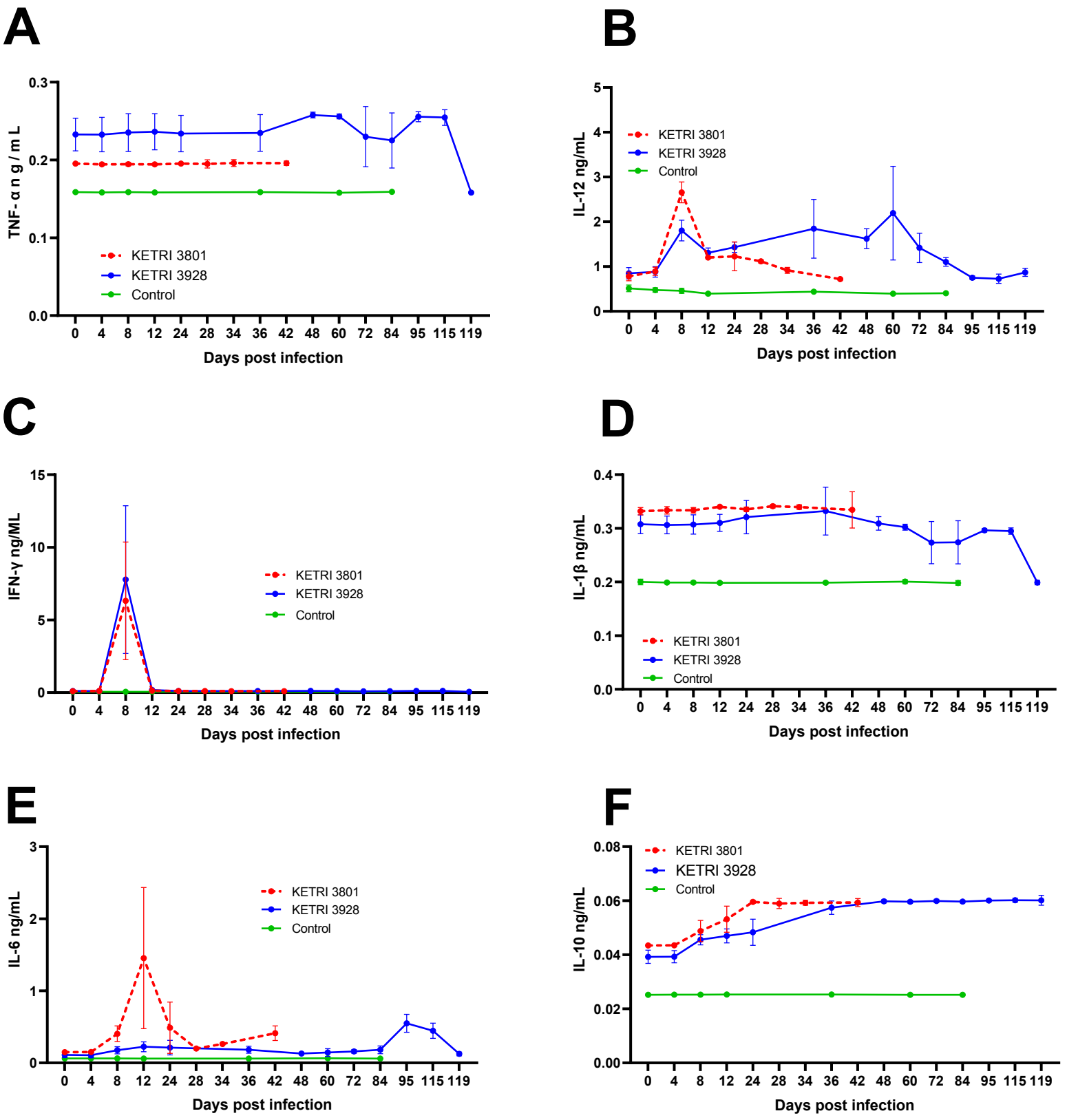

Figure 4. Plasma cytokine alterations in the course of *T. b. rhodesiense* infection of vervet monkey. Graphs showing changes of cytokines in the course of tsetse-mediated infection of vervet monkeys with two strains of *T. b. rhodesiense* KETRI 3801 and KETRI 3928. The respective host immune factors were monitored till extremis for KETRI 3801 infection and termination of experiment for KETRI 3928 infection and control.

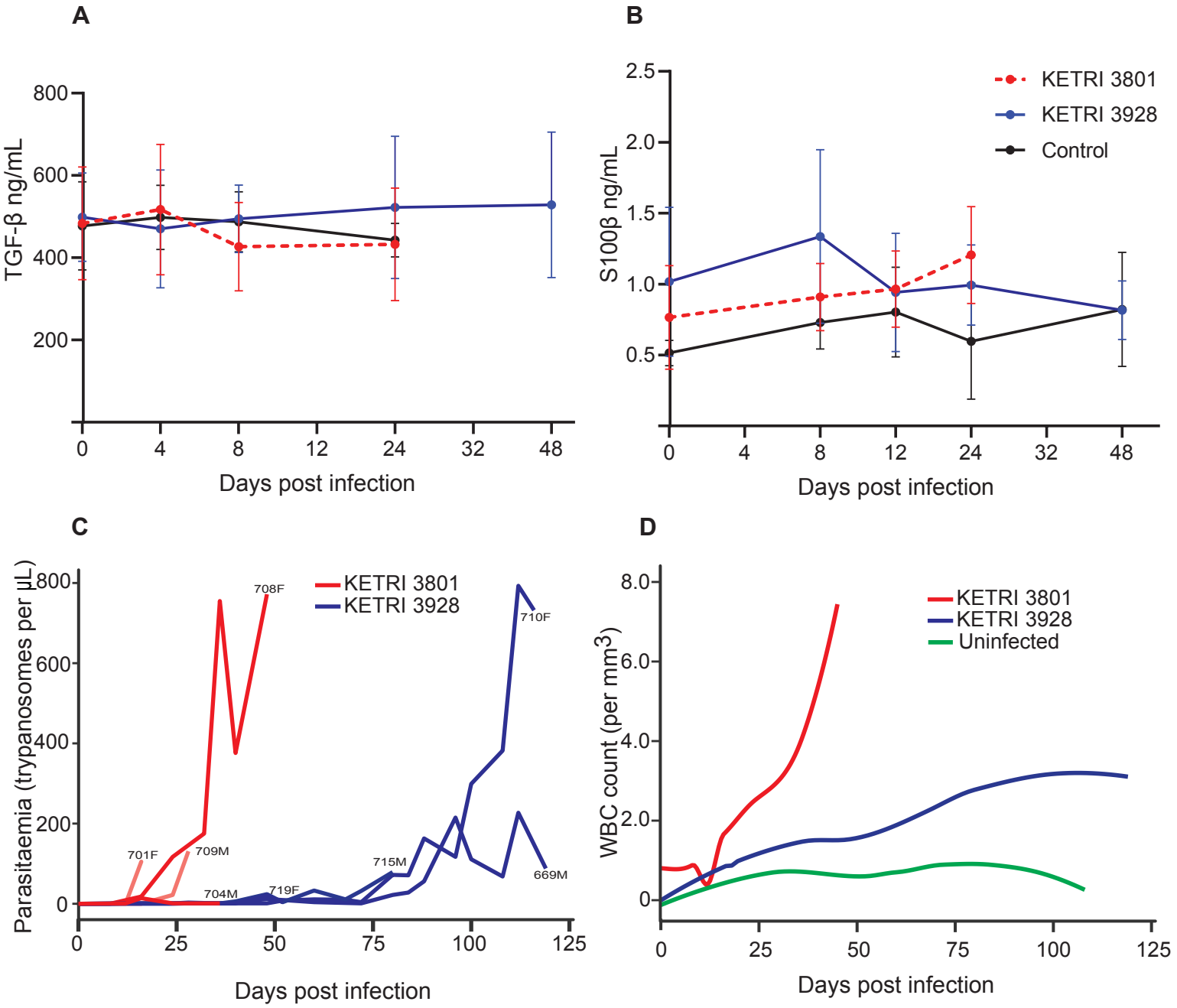

Figure 5. Cerebrospinal fluid (CSF) trypanosome invasion and associated immune factors levels in the course of infection of vervet monkeys with *T. b. rhodesiense* strains. A. Graphs showing the profile of TGF-β and **B.** S100β in ng/ml in the early stages of tsetse-mediated infection of vervet monkeys with two strains of *T. b. rhodesiense* KETRI 3801 and KETRI 3928. **C.** Both parasite strains cross the blood brain barrier (BBB) into the CSF causing stage 2 disease in all the infected animals. **D**. The invasion is accompanied by increase in CSF white blood cell (WBC) count as shown by the trend. The graph is an illustration of the averages of the members of each cohort. The numbers in figure C represent the codes for individual infected animals.

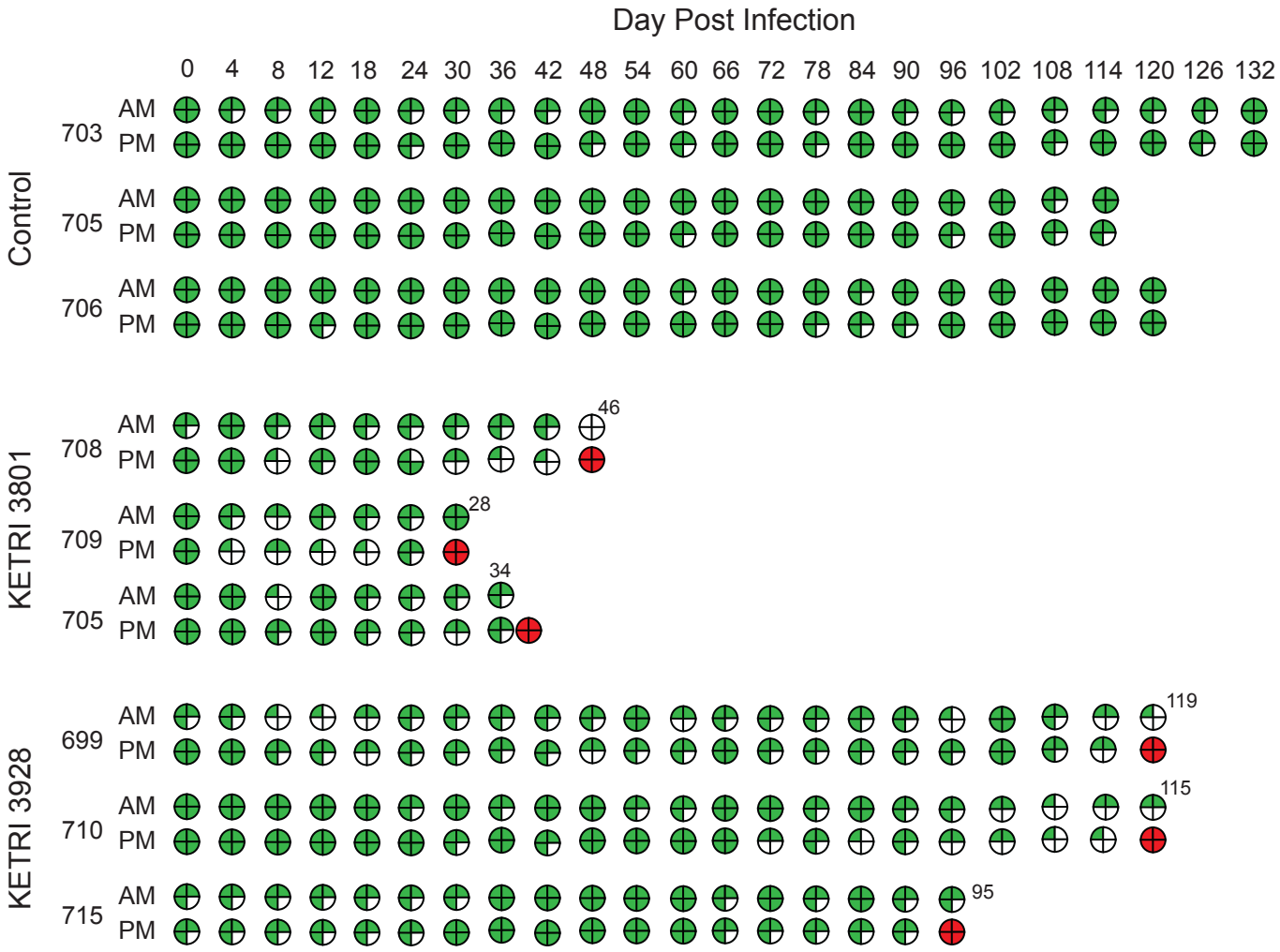

Figure S1. Hypophagia observed in vervet monkey infected with KETRI 3801 and KETRI 3928 strains of *T. b. rhodesiense.* The animals were fed on maize cobs, carrots, bananas and commercial pellets. The amount of food consumed was estimated, allowing inferance of appetite and hypophagia as illustrated here. Here, ⊕ : fed on all food items provided; ◕: three quarter consumed; ◑ : a half consumed; ◔: a quarter consumed and finally ⊕: animal did not feed. ⊕ represents extremis, with day post-infection indicated as superscript for each infected aniamal. Animals eating just a quarter and below were clearly anorexic.

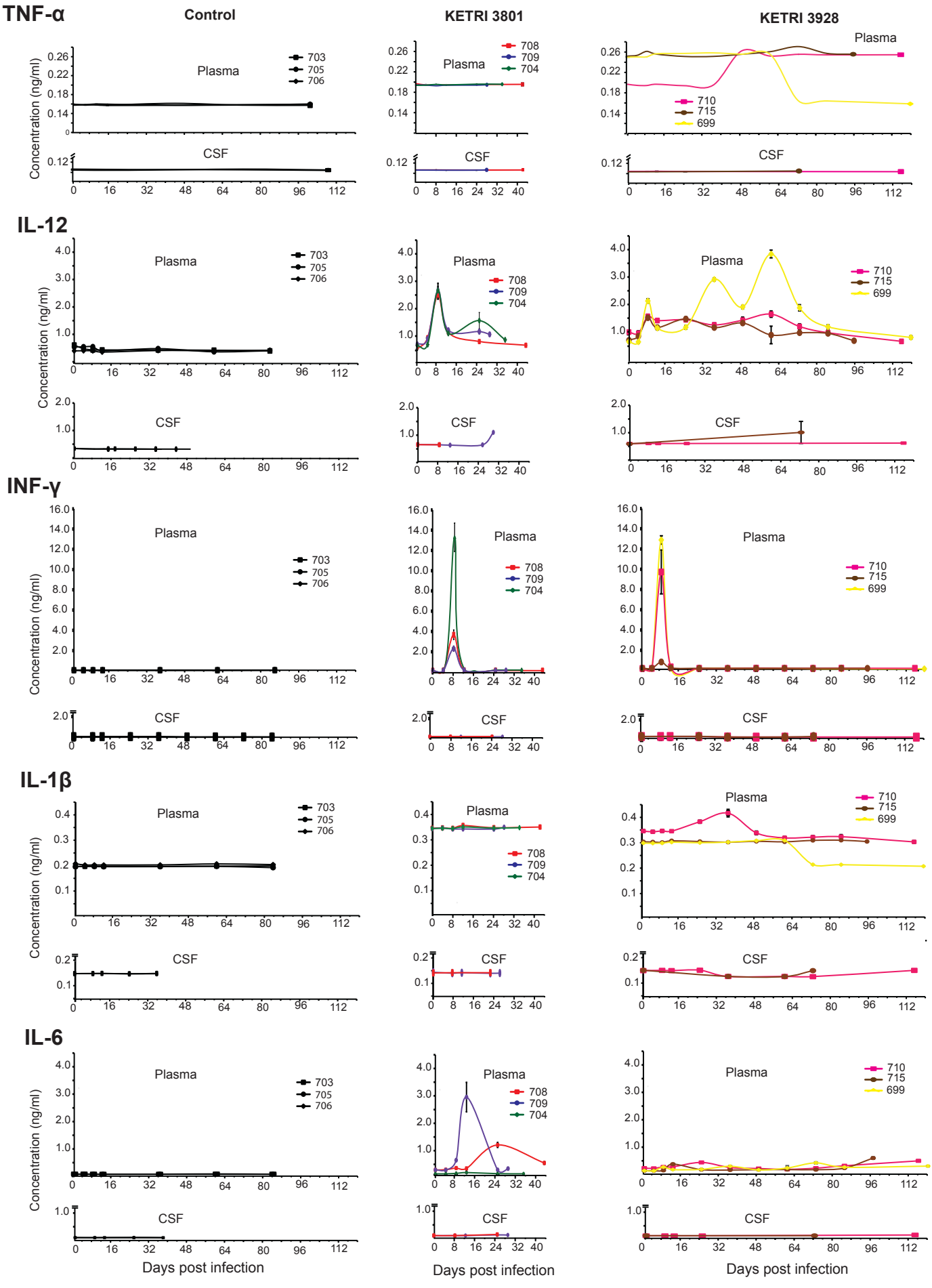
TNF-α
Control
KETRI 3801
KETRI 3928
IL-12
INF-γ
IL-1β
IL-6
Plasma
CSF
Concentration (ng/ml)
703
705
706
708
709
704
710
715
699
Days post infection

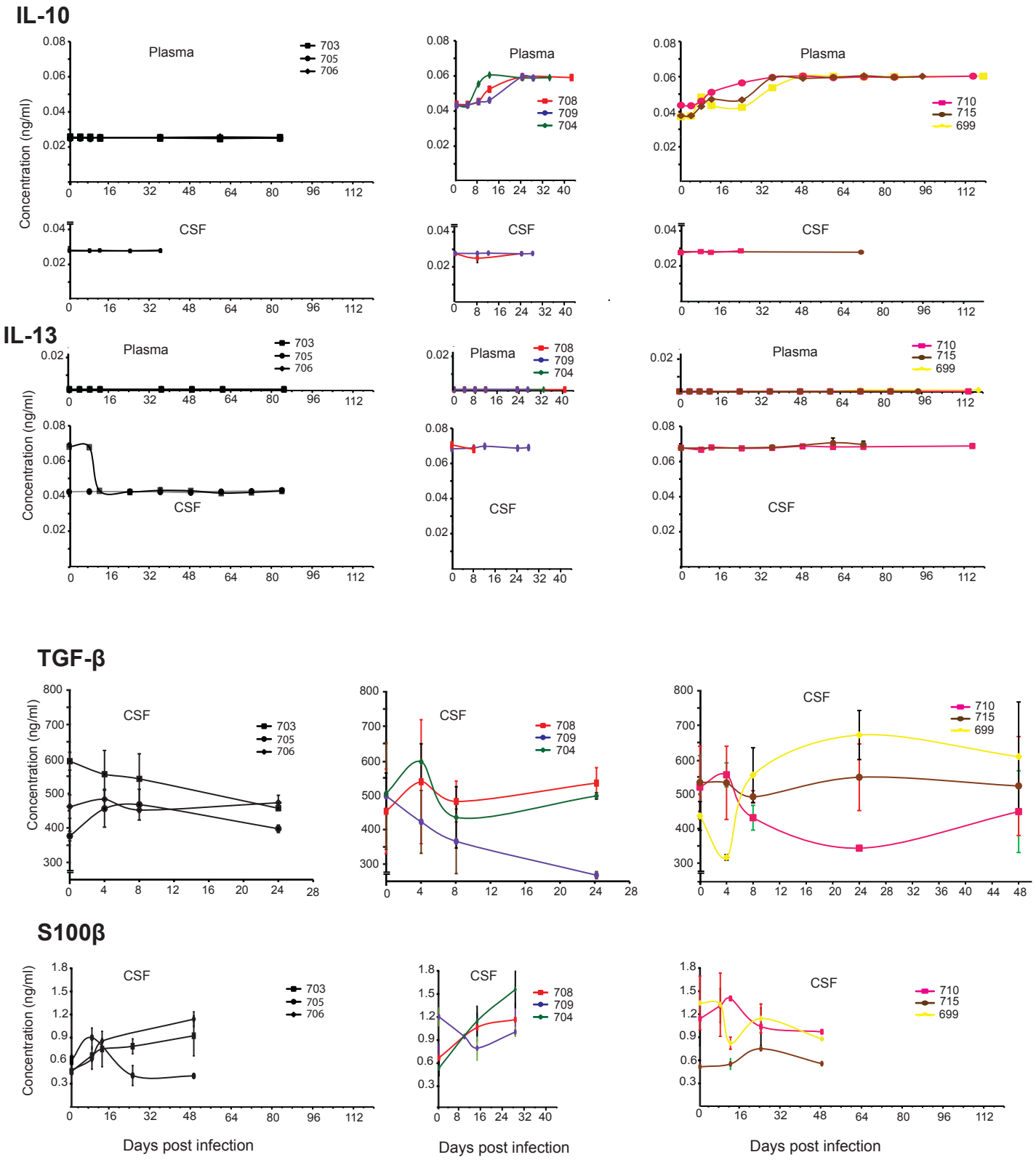

Figure S2. Plasma and cerebrospinal fluid (CSF) cytokine and S100β changes in the course of *T. b. rhodesiense* infection of veret monkey. Graphs showing changes of cytokines in plasma and CSF in the course of tsetse-mediated infection of individual vervet monkeys with two strains of *T. b. rhodesiense* KETRI 3801 and KETRI 3928. The respective host immune factors and brain damage biomarker S100β were monitored till extremis for KETRI 3801 infection and termination of experiment for KETRI 3928 infection and control. The individual animals were given number cords and profiles shown in the respective colors.

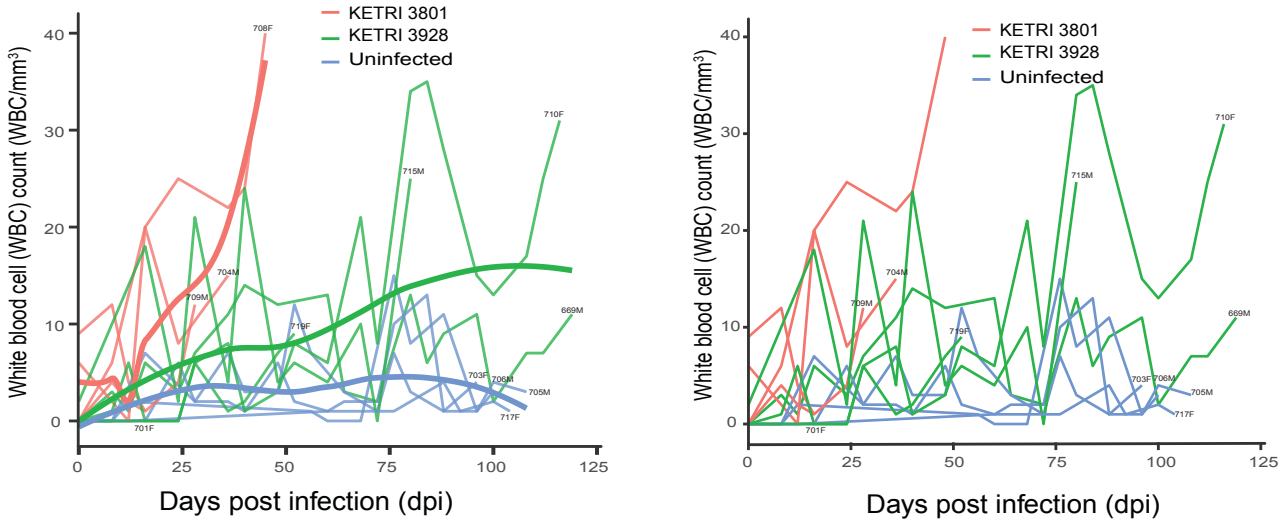

Figure S3. Cerebrospinal fluid (CBF) white blood cell (WBC) count. Parasite invasion of the central nervous system (CNS) is accompanied by increase in CSF white blood cell (WBC) count as shown by the trend. The graph is an illustration of the averages of the members of each cohort. The numbers represent the codes for individual animals, and the bolder lines the avaerage than is smoothened and not.

849

850